

Ship Navigation Effect on Sedimentation in Restricted Waterways

M. Nakisa^a, A. Maimun^{b*}, Yasser M. Ahmed^a, F. Behrouzi^a, Jaswar Koto^a, A. Priyanto^a, A. Y. Sian^a, S. A. Ghazanfari^a

^aFaculty of Mechanical Engineering, Universiti Teknologi Malaysia, 81310 UTM Johor Bahru, Johor, Malaysia

^bMarine Technology Centre, Universiti Teknologi Malaysia, 81310 UTM Johor Bahru, Johor, Malaysia

*Corresponding author: adi@fkm.utm.my

Article history

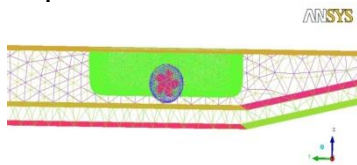
Received :12 November 2013

Received in revised form :

28 March 2014

Accepted :1 April 2014

Graphical abstract



Meshing of soil erosion in confined water

Abstract

This research work has focused on the environmental soil erosion in restricted water. The sedimentation is occurred by ship bank interaction phenomenon. Computational Fluid Dynamics (CFD) is used to predict the soil erosion as a major global environmental issues. These kind of issues are referring to increase the precipitation of canals, environmental degradation, and non-specific source of contamination. Therefore, it is important to understand the processes of soil erosion and sediment transport along rivers. This can potentially help to identify the erosion vulnerable areas and find potential measures to reduce the environmental effects. The merchant ships such as LNG carriers, Ro-Ro ships and general cargo carriers navigate through the restricted waterways that have significant effects on soil erosion. In this study, we investigated the soil erosion and identified the most seriously eroded areas in the confined waterways via Finite Volume Method (FVM).

Keywords: Environmental soil erosion; CFD; Restricted water; LNG carrier

© 2014 Penerbit UTM Press. All rights reserved.

1.0 INTRODUCTION

Fluvial erosion is considered to be the most common bank erosion process in many rivers. However, in many instances the actual bank failure occurs long after the high stage flow period and in places which are not affected by fluvial erosion.¹⁻²

This indicates that other processes, such as seepage induced erosion of river banks, are also important mechanisms for bank failure.³⁻⁷ Mass wasting processes of hillslopes and stream-banks due to subsurface flow, which is essentially seepage gradient forces and preferential flow through soil pipes is reviewed.⁸⁻⁹ However, due to complexity of the interactive effects of surface flow, seepage and pipe flow and presence of vegetation, further study is necessary. The interaction among the mass failure, bank hydrology and other hydrological factors related to river hydrograph were focused.⁵⁻⁶ They pointed out that periods of high river stage changes the pore water pressure within riverbanks due to flow from the river into the banks called bank storage. This increased pore water pressure was recognized as the most important factor for mass failure. Flume studies pointed out that erosion rates of the bank surface increase in magnitude when the unsaturated pore water pressure is near to saturation and soil strength is decreased.⁸⁻⁹

Seepage erosion involved soil particles entrained with infiltrated water from the river bank to form a zone of seepage undercut. Consequently, failure of the overhanging bank mass occurs.¹⁹ In composite river banks, like the Brahmaputra, seepage erosion mainly occurs because of the presence of sand layers between the fine soil layers, which permits high rates of seepage flow.¹⁰ High rainfall infiltration rate causes the development of a perched water table above the less permeable layers.

Subsequently, large hydraulic gradient of the flow initiates towards stream channels causing fairly rapid subsurface flow.²³

Various conditions required for seepage erosion. The most important conditions are the presence of the open exfiltration face, source of water which can create sufficient water head, removal of failed or displaced materials from the bank toe and a sufficient hydraulic gradient. A composite river bank often provides an open exfiltration face. During the rising phases of the stage hydrograph, the water from the river infiltrates through the bank face and stored as bank storage.¹⁰ However, in the receding phase, this stored water returns back to the river through the high conductivity layer with high seepage velocity, which causes the seepage erosion. Other sources of seepage are lateral flow due to presence of perched water table due to rainfall infiltration in the alluvial plains or even uplands.¹¹⁻¹² Subsequent removal of displaced seepage materials from its site of origin is important for further seepage erosion.¹³⁻¹⁴

Many researchers investigated the role of seepage on erosion for hillslope stability and bank erosion. It has been reported that the seepage pressure acts as a body force on representative sediment volume.¹⁵⁻¹⁷ Erosion of cohesionless soil particles from the river bank faces by groundwater occurs under the influence of three forces: tractive force defined as the sum of all external forces acting on the seepage face, gravity force, and seepage force exerted by the groundwater on the sediment grain. The seepage force is:

$$F_s = C_2'' \cdot 3\pi/n (\rho_f \cdot g \cdot i \cdot d^2) \quad (1)$$

Where ρ_f is the fluid density, g is the acceleration due to gravity, d is the median grain size, C_2'' is an empirical constant, i is

the hydraulic gradient, and n is the porosity. Seepage force dominates in a narrow sapping zone at the seepage outflow point and erosion occurs thereafter as a continuous outward sediment movement through this zone. The under cutting subsequently initiates failure of the undermining zone which is above the seeping zone.¹⁸⁻¹⁹

A number of researchers studied river bank erosion processes by measuring seepage erosion rate and soil–water pressure^{12,16,20}. A long term sediment delivery flux, which depends on the critical failure angle of the bank materials are proposed.¹⁸⁻¹⁹ In recent studies, bank failure models also included seepage erosion phenomenon in a stratified river bank.^{13,17,21} Out laboratory experiments on a sandy-gravel river bank model was carried to investigate the basic processes of seepage erosion due to variation of river stage. Their results indicated that erosion and failure of bank was due to loss of matric suction resulting in cantilever, slab and slide failure during ascending phase of the hydrograph.¹⁹The following power relationship between the seepage erosion rate and flow discharge is suggested:

$$E = aQ^2 \tag{2}$$

Where E is the seepage erosion rate, Q is the flow discharge and a is the regression parameter.^{14,18} Based on the theory of seepage erosion, a dimensionless sediment transport model had been proposed by normalizing the bank slope, bank soil profile depth, and boundary conditions of the lysimeter experiments. The dimensionless sediment discharge(q_s^*) and the dimensionless shear stress (τ^*) are related through the following power relationship:¹¹

$$q_s^* = 584 \times \tau^{*1.04} \tag{3}$$

The above equation can be applied to actual field conditions. This equation is quite similar to the empirical bed load function for fluvial erosion.²¹⁻²³ An apparatus was developed to investigate three dimensional seepage erosion mechanisms of the river bank face or hillslope in laboratory.²³

The experimental results showed similar power relationship between the magnitude of erosion and the height of undercut of the bank. It is extremely important to apply the experimentally developed relationships between the available seepage gradient and the bank erosion rate at the river scale. However, no study to date has been carried out to characterize the seepage behavior for composite river banks and prediction of the seepage erosion and subsequent bank retreat. In some limited laboratory studies attempts have been made to establish a relationship between the seepage head and the sediment discharge rate from composite river banks.²²⁻²⁵

A function of time required for seepage undercutting in relation with the soil cohesion, bulk density, and the hydraulic gradient in the near bank ground water system.²³ The influences of bank angles on seepage erosion was studied.²⁸ Sensitivity study of the soil hydraulic properties on seepage erosion was carried out for numerical prediction of the seepage gradient forces.¹¹ Four different bulbous bows fitted to a catamaran $s/L = 0.2$ were tested in waterdepth 400 mm at speed range 1–4 m/s to measure the total resistance, trim, sinkage and wave elevation or wash.²⁹In situ constant head experiments was conducted to investigate seepage-induced bank erosion and instability on the streambank of Dry Creek in Mississippi. Heterogeneous natural bank stratification consisted of conductive loamy sand layers between cohesive layers. They concluded that the seepage erosion, linked with fluvial erosion, can be an important mechanism for streambank erosion.¹⁵

2.0 STUDY AREA

As problem statement, the Rajang River in Malaysia is typically braided and complex in the planform (Figure 1-2). Rajang River runs through in the middle of the state of Sarawak. The river is the longest and the largest in Malaysia; it is 760 km in length and has a drainage area of 50,000 km². The headstream is located in Iran Mountains that divides the state of Sarawak and Indonesia. The river runs into the center part of the state and reaches the South China Sea. The study area is covered by Paleogene mudstone.

The main ridge along with the strike of bed stretches in the east-west by the pressure from north-south direction of the Indo-Australian Plate movement. Thus, Rajang River runs along the subsequent valley. The river is very commonly known for its high bank erosion hazards. The average annual rainfall is about 1600 mm in this Rajang River basin.²⁶⁻²⁷

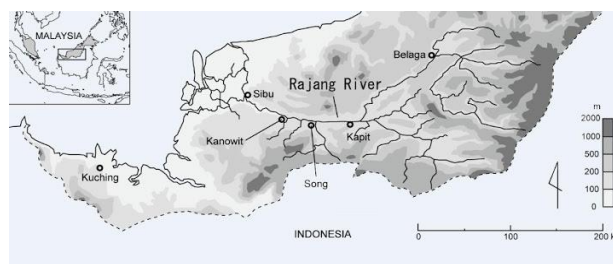


Figure 1 The Rajang River Basin



Figure 2 The Rajang River soil erosion

3.0 MODELING

The ship and propeller model studied in this paper for numerical simulations and experiments is a Tenaga Class Liquefied Natural Gas (LNG) tanker, at scale of 1/80. The principal dimensions and the lines of the ship body plan are shown in Table 1, Figure 3 and Table 2.

Table 1 Principal dimensions of the LNG vessel

	Full scale	Model
L_{tp} (m)	266	3.325
Beam (m)	41.3	0.51625
Draft (m)	11.13	0.139125
Block coefficient, C_b	0.746	0.746
Wetted surface area (m ²)	14032.66	1.53

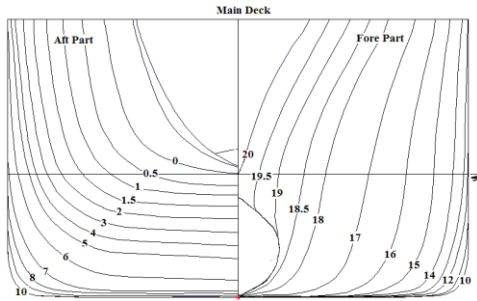


Figure 3 Body plan of the LNG ship

Same Froude number in model and full scale ensures the model and full-scale ships exhibit similar behavior. In general, the Froude number, F_n , is defined as:

$$F_n = V / \sqrt{gL_{wl}} \tag{4}$$

Where V is the velocity of the ship, g is the acceleration due to gravity, and L_{wl} is the length of the ship at waterline level.

Table 2 Propeller geometric characteristics

Parameters	Dimension
Z	5
D	7.7 m
Dhob	1.28 m
Br	0.17
P/D	0.94
Ae/A0	0.88
R	15 Deg.

4.0 NUMERICAL SIMULATION

The numerical predictions presented in this work were carried out with the ANSYS-CFX, commercial CFD solver. It employs the node-centered finite volume method. Figure 4 and Figure 5 show the schemes and mesh information for simulation the LNG carrier in restricted water (bank-shallow water with sand).

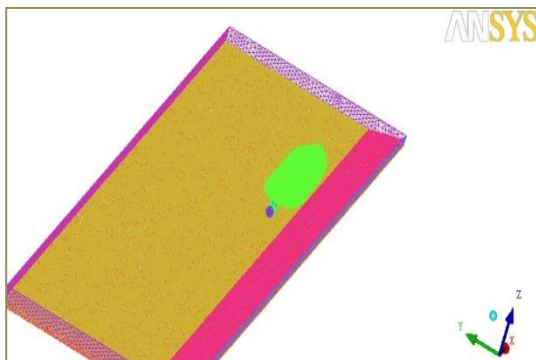


Figure 4 Numerical domain with sand bank-shallow water

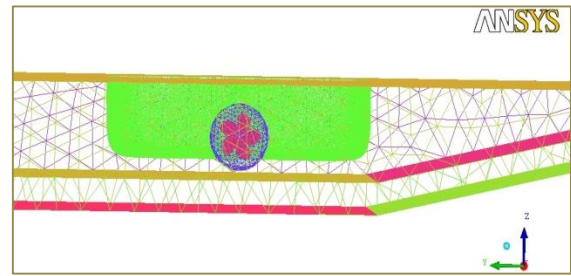


Figure 5 Numerical domain with sand-restricted water

5.0 GOVERNING EQUATIONS

In Cartesian tensor form the general RANS equation for continuity can be written as,

$$\frac{\partial \rho}{\partial t} + \frac{\partial(\rho u_i)}{\partial x_i} = 0 \tag{5}$$

and equation for momentum become:

$$\begin{aligned} \frac{\partial(\rho u_i)}{\partial t} + \frac{\partial(\rho u_j u_i)}{\partial x_j} = & \\ -\frac{\partial \rho}{\partial x_i} + \frac{\partial}{\partial x_i} [\mu (\frac{\partial u_i}{\partial x_j} + \frac{\partial u_j}{\partial x_i} - \frac{2}{3} \delta_{ij} \frac{\partial u_k}{\partial x_k})] + & \\ \frac{\partial}{\partial x_i} (-\rho \overline{u_i u_j}) + f_{bi} & \end{aligned} \tag{6}$$

In the above equation u_i is i th Cartesian component of total velocity vector, μ is molecular viscosity, $(-\rho \overline{u_i u_j})$ is Reynolds stress, δ_{ij} is Kronecker delta and p is static pressure. The Reynolds stress should be demonstrated to near the governing equations by suitable turbulent model. For solution the RANS equation and turbulence velocity time scale, it is used by Boussinesq's eddy-viscosity supposition and two transport equations. The body force is expressed by f_{bi} .

For determination the 3D viscous incompressible flow around the ship's hull is used the ANSYS-CFX14.0 code. The parallel version of CFX concurrently calculates the flow formulations using numerous cores of computers. The shear stress transport (SST) turbulence model had been used in this study, because it gave the best results in comparison with other turbulence models. The equations are shown as follows:

Equation of k :

$$\frac{\partial}{\partial t} (\rho k) + \frac{\partial}{\partial x_i} (\rho k u_i) = \frac{\partial}{\partial x_j} (\Gamma_k \frac{\partial k}{\partial x_j}) + G_k - Y_k + S_k \tag{7}$$

Equation of ω :

$$\frac{\partial}{\partial t} (\rho \omega) + \frac{\partial}{\partial x_i} (\rho \omega u_i) = \frac{\partial}{\partial x_j} (\Gamma_\omega \frac{\partial \omega}{\partial x_j}) + G_\omega - Y_\omega + S_\omega \tag{8}$$

Where G_k and G_ω express the generation of turbulence kinetic energy due to mean velocity gradients and ω . Γ_k and Γ_ω express the active diffusivity of k and ω . Y_k and Y_ω represent the dissipation of k and ω due to turbulence. D_ω expresses the cross-

diffusion term, S_k and S_ω are user-defined source terms Further detail is available.⁹

6.0 RESULT AND DISCUSSION

A series of model experiments to measure the ship-bank interactive forces were conducted to validate the numerical calculations. The experiments were conducted in the towing tank at Marine Technology Centre (MTC) of Universiti Teknologi Malaysia (UTM) which is showed in Figure 6.



Figure 6 Ship model in testing situation with bank-shallow water

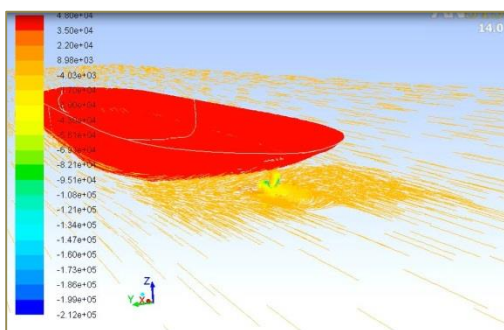


Figure 7 Flowspeed at propeller zone

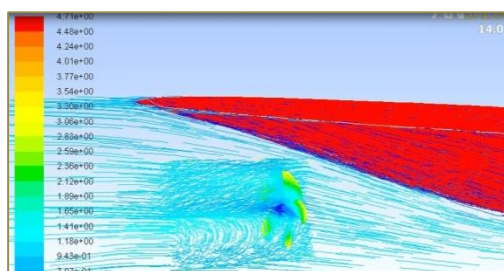


Figure 8 Accumulated flow velocity streamlines at propeller face

Figures 7-8 are showing the flow streamlines directions affected by working propeller behind the ship. Stern ship specially propeller zone is very important and considered to suitable design for converging the streamlines into the propeller plane. In this regions the soil erosion and sedimentation will be occurred due to more suction under and band side of the hull ship and also propeller zone.

It is noticed that for a given ship-bank distance, the bank effect increase with higher of ship speed. In general, the bank

effect reduces with increase of ship-bank distance and lower ship speed.

7.0 CONCLUSION

CFD simulations and experiments have been conducted for bank effect on soil erosion acting on a LNG tanker in restricted water condition. In according to the presented computational results based on RANS equations, the following conclusions are taken:

- The proximity of bank and shallow water has a significant effect on the hydrodynamic pressure and velocity contours around the ship hull therefore the soil erosion will be occurred at the restricted waterways.
- The hydrodynamic interactive force and moment increase with reducing of ship-bank distance. For a given ship bank distance, the bank effect is more pronounce with an increasing of ship speed.
- In according to high velocity under the bottom in shallow water, it might be caused to sink the hull to the sea bed.

Acknowledgements

The authors would like to express their sincere gratitude to MOHE-UTM- vote No. 4F321 (Universiti Teknologi Malaysia-UTM) for its supporting of this research project.

Nomenclature

D	: Propeller diameter, (m)
D_{hub}	: Hub diameter, (m)
Z	: Number of blade
P/D	: Pitch Ratio
R	: Rake of Blades
N	: Rate of revolutions of propeller, (rpm)
C_p	: Pressure coefficient
P	: Static pressure at point of interest
p_0	: Reference pressure at infinity
Va	: Advance velocity, (m/s)
J	: Advance ratio
KT	: Thrust coefficient
KQ	: Torque coefficient
Br	: Boss ratio
A_E/A_0	: Expanded Area Ratio (EAR)
ρ	: Density of water
η	: Open water efficiency
D_r	: Diameter of Rotational domain
L_r	: Length of rotational domain
L_{mr}	: Outlet length of rotational domain
D_s	: Diameter of stationary domain
L_{so}	: Length of outlet stationary domain
L_{si}	: Length of inlet stationary domain
(x, y, z)	: Cartesian coordinate system with its origin at the centre of propeller
+X, +Y, +Z	: Cartesian directions in Right-Hand system
U_x, U_y, U_z	: Velocity components in the Cartesian

References

- [1] D. J. Hagerty. 1991a. Piping/sapping Erosion-1: Basic Considerations. *J. Hydraul. Eng.* 117(8): 991–1008.
- [2] D. J. Hagerty. 1991b. Piping/sapping Erosion-2: Identification Diagnosis. *J. Hydraul.*

- [3] S. E. Darby, C. R. Thorne. 1996. Numerical Simulation of Widening and Bed Deformation of Straight Sand-bed Rivers. I: Model Development. *J. Hydraul. Eng. ASCE*. 122(4): 184–193. K. Elissa, Title of paper if known, unpublished.
- [4] G. Crosta, C. di Prisco. 1999. On Slope Instability Induced by Seepage Erosion. *Can. J. Geotech. Eng.* 36: 1056–1073.
- [5] M. Rinaldi, N. Casagli. 1999. Stability of Streambanks Formed in Partially Saturated Soils and Effects of Negative Pore Water Pressures: The Siene River (Italy). *Geomorphology*. 26(4): 253–277.
- [6] M. Rinaldi, L. Nardi. Modeling Interactions Between River Hydrology and Mass Failures. *J. Hydrol. Eng.* In press.
- [7] D. L. Rockwell. 2002. The Influence of Groundwater on Surface Flow Erosion Processes. *Earth Surf. Processes Landf.* 27(5): 495–514.
- [8] G. A. Fox, G. V. Wilson. 2010. The Role of Subsurface Flow in Hillslope and Stream Bank Erosion: A Review. *Soil Sci. Soc. Am. J.* 74(3): 717–733.
- [9] G. A. Fox, G. V. Wilson, R. K. Periketi, B. F. Cullum. 2006. A Sediment Transport Model for Seepage Erosion of Streambanks. *J. Hydrol. Eng.* 11(6): 603–611.
- [10] G. A. Fox, G. V. Wilson, A. Simon, E. Langendoen, O. Akay, J. W. Fuchs. 2007. Measuring Streambank Erosion Due to Ground Water Seepage: Correlation to Bank Pore Water Pressure, Precipitation and Stream Stage. *Earth Surf. Processes Landf.* 32: 1558–1573.
- [11] G. A. Fox, D. M. Heeren, G. V. Wilson, E. J. Langendoen, A. K. Fox, M. L. Chu-Agor. 2010. Numerically Predicting Seepage Gradient Forces and Erosion: Sensitivity to Soil Hydraulic Properties. *J. Hydrol.* 389: 354–362.
- [12] O. L. Owoputi, W. J. Stolte. 2001. The Role of Seepage in Erodibility. *Hydrol. Process.* 15(1): 13–22.
- [13] D. L. Rockwell. 2002. The Influence of Groundwater on Surface Flow Erosion Processes. *Earth Surf. Processes Landf.* 27(5): 495–514.
- [14] R. C. Kochel, A. D. Howard, D. F. McLane. 1985. Channel Networks Developed by Groundwater Sapping in Fine-grained Sediments: Analogs to Some Martian Valleys. In: Woldenberg, M. J. (Ed.), *Models in Geomorphology*. Allen and Unwin, Boston. 313–341.
- [15] T. L. Midgley, G. A. Fox, G. V. Wilson, D. M. Heeren, E. J. Langendoen, A. Simon. 2012. Seepage-induced Streambank Erosion and Instability: In-Situ Constant Head Experiments. *J. Hydrol. Engrg.* doi: 10.1061/(ASCE)HE 1943- 6584.0000685.
- [16] K. Terzaghi. 1943. *Theoretical Soil Mechanics*. Wiley, New York. Van Genuchten, M.Th. 1980. A Closed-form Equation for Predicting the Hydraulic Conductivity of Unsaturated Soils. *Soil Sci. Soc. Am. J.* 44(5): 892–898.
- [17] D. Zaslavsky, G. Kassiff. 1965. Theoretical Formulation of Piping Mechanisms in Cohesive Soils. *Geo-technique*. 15(3): 305–316.
- [18] A. D. Howard, C. F. McLane. 1988. Erosion of Cohesionless Sediment by Ground Water Seepage. *Water Resour. Res.* 24(10): 1659–1674.
- [19] L. Nardi, M. Rinaldi, L. Solari. 2012. An Experimental Investigation on Mass Failures Occurring in a Riverbank Composed of Sandy Gravel. *Geomorphology*. 163–164: 56–69.
- [20] E. Meyer-Peter, R. Muller. 1948. Formulas for Bed Load Transport. In: Proc. Second Meeting Int. Assoc. Hydraul. Res. Stockholm, Sweden. 39–64.
- [21] J. M. Nelson, J. D. Smith. 1989. Evolution and Stability of Erodible Channel Beds. In: Ikeda, S., Parker, G. (Eds.), *River Meandering, Water Resources Monograph Series*, vol. 12. American Geophysical Union, Washington, D.C.
- [22] Istanbulluoglu, E., Tarboton, D. G., Pack, R. T., Luce, C. 2003. A Sediment Transport Model for Incising Gullies on Steep Topography. *Water Resour. Res.* 39(4): 1103.
- [23] M. L. Chu-Agor, G. A. Fox, R. M. Cancienne, G. V. Wilson. 2008. Seepage Caused Tension Failures and Erosion Undercutting of Hillslopes. *J. Hydrol.* 359: 247–259.
- [24] K. Yuhora, S. Ryoji, M. Kuniyasu. 2009. Bank Erosion along the Rajang River and Its Social Impacts. *Geographical Studies*. 84: 23–35.
- [25] J. M. Nelson, J. D. Smith. 1989. Evolution and Stability of Erodible Channel Beds. In: Ikeda, S., Parker, G. (Eds.), *River Meandering, Water Resources Monograph Series*, vol. 12. American Geophysical Union, Washington, D.C.
- [26] E. Istanbulluoglu, D. G. Tarboton, R. T. Pack, C. Luce. 2003. A Sediment Transport Model for Incising Gullies on Steep Topography. *Water Resour. Res.* 39(4): 1103.
- [27] M. L. Chu-Agor, G. A. Fox, R. M. Cancienne, G. V. Wilson. 2008. Seepage Caused Tension Failures and Erosion Undercutting of Hillslopes. *J. Hydrol.* 359: 247–259.
- [28] N. Lindow, G. A. Fox, R. O. Evans. 2009. Seepage Erosion in Layered Stream Bank Material. *Earth Surf. Processes Landf.* 34: 1693–1701.
- [29] M. P. Abdul Ghani, P. A. Wilson. 2009. Experimental Analysis of Catamaran Forms with Bulbousbows Operating in Shallow Water. *International Shipbuilding Progress*. 56: 29–57.